POLITECNICO DI TORINO
Repository ISTITUZIONALE

Estimation of PM Machine Efficiency Maps from Limited Experimental Data

Original
Estimation of PM Machine Efficiency Maps from Limited Experimental Data / Kahourzade, S., Mahmoudi, A., Soong, W.L., Ertugrul, N., Pellegrino, G.. - STAMPA. - (2018), pp. 4315-4322. (10th Annual IEEE Energy Conversion Congress and Exposition, ECCE 2018 Portland (USA) 2018) [10.1109/ECCE.2018.8557885].

Availability:
This version is available at: 11583/2727543 since: 2019-03-08T09:26:13Z

Publisher:
Institute of Electrical and Electronics Engineers Inc.

Published
DOI:10.1109/ECCE.2018.8557885

Terms of use:

This article is made available under terms and conditions as specified in the corresponding bibliographic description in the repository

Publisher copyright
IEEE postprint/Author's Accepted Manuscript

©2018 IEEE. Personal use of this material is permitted. Permission from IEEE must be obtained for all other uses, in any current or future media, including reprinting/republishing this material for advertising or promotional purposes, creating new collecting works, for resale or lists, or reuse of any copyrighted component of this work in other works.

(Article begins on next page)

26 November 2026

Estimation of PM Machine Efficiency Maps From Limited Experimental Data

Solmaz Kahourzade[1], Amin Mahmoudi MIEEE[2,*], Wen L. Soong MIEEE[1], Nesimi Ertugrul MIEEE[1], and Gianmario Pellegrino[3]

[1]School of Electrical and Electronic Engineering, University of Adelaide, Australia
[2]College of Science and Engineering, Flinders University, Australia
[3]Politecnico di Torino, Corso Duca degli, Abruzzi 24, Torino, 10129 Italy
*Corresponding Author: amin.mahmoudi@flinders.edu.au

***Abstract*— This paper investigates the accuracy of the estimation of efficiency maps for permanent magnet (PM) machines using the *d-q* equivalent circuit model and limited experimental data. The study is based on the detailed finite-element results for 50-kW surface and interior PM machines. It discusses the variation of the flux-linkages and losses with I_d and I_q. It examines the effect of modeling the flux-linkage characteristics using saturating and linear models and modelling the non-copper losses using the open-circuit and short-circuit losses. The effect of these approximations on the output torque versus speed capability curve and efficiency contours are shown. Guidelines are proposed for fast and reasonably accurate calculation of efficiency maps.**

***Keywords*— Efficiency maps, loss modeling, permanent magnet machines.**

I. INTRODUCTION

Efficiency maps are commonly used to graphically illustrate and compare the performance of electric machines. They are contour plots of maximum efficiency on axes of torque (or power) versus speed. Efficiency maps show not only the capability envelope of the machine but also the efficiency at all possible operating points.

The most accurate means to obtain these are based on experimental tests or finite element (FE) simulations. Experimentally this requires the availability of a sophisticated and accurate test arrangement while FE analysis requires extensive computation time and data processing. Improved computational capabilities has helped FE analysis but experimental measurement of efficiency maps is still challenging.

This paper focusses on an important problem which has received limited attention in the literature: examining the accuracy of estimating efficiency maps using limited experimental measurements such as the stator resistance, inductances and the open and short-circuit losses. This investigation is performed using an extensive set of finite-element loss and flux-linkage data for example 50-kW surface and interior PM machines.

Even though efficiency maps are commonly used, there is limited published work addressing the trade-off between the accuracy and effort of the calculation techniques. A successful calculation of the efficiency maps for electrical machines relies on accurate flux linkage and loss determination. Finite-element analysis is considered the most precise method to calculate the efficiency map that considers the machine's non-linearities, hysteresis and eddy-current losses [1]. It requires significant post-processing which includes loss data analysis for each torque-speed point in the T-ω plane. The alternative method is analytical calculation based on the equivalent circuit data and simplified loss model which mostly considers the non-copper loss as a function speed only [2, 3]. These simplifying assumptions result in a coarse estimation of efficiency map which can be improved by considering the impacts of saturation and cross coupling [4].

This paper was inspired from the desire to obtain a reasonably accurate efficiency map based on the available motor data and simple tests. It seeks to fill this gap by examining the alternative methods of efficiency map calculation applicable for any machine topology. An improvement to previously published literature is a detailed discussion on the key PM machine characteristics (flux and losses) with operating points (I_d, I_q). A contribution of this work is investigation of the efficiency map calculation based on flux and loss approximations. It considers accounting the non-copper losses of the machine from open-circuit and short-circuit loss tests and nonlinear behaviours of flux linkage while investigating both cross-saturation, saturation, and linear behaviours. The flux linkage and loss contours are presented and hence the optimal control trajectory in the I_d-I_q plane and the effects of such approximations on operational envelopes and efficiency contours are investigated.

II. THEORETICAL FRAMEWORK

The efficiency map shows the maximum machine efficiency at a given torque/speed point that satisfies the machine constraints including voltage limit (usually set by the power converter DC bus voltage) and current limit (usually set by the machine/inverter thermal limits) (see Fig. 1a). Brushless PM machines normally use *d*- and *q*-axis current control to achieve smooth torque control and fast dynamic response. For a given speed, all combinations of I_d and I_q which produce the required torque (see Fig. 1b) and are compatible with both voltage and current constraints are considered (see Fig. 1c). Among those, the I_d and I_q combination resulting in the highest efficiency (lowest loss) is chosen to produce a single point on the efficiency map (see Fig. 1d). The process is repeated covering the entire torque versus speed domain.

There are three methods to obtain the efficiency maps: equivalent circuit, finite-element (FE) simulation, and experiment measurement. Excluding the experimental testing (which involves the practical measurement of the efficiency map), the FE simulation and the equivalent circuit methods require knowledge of flux linkage and iron loss variations as a function of the I_d and I_q currents.

A. Equivalent Circuit

The equivalent circuit method is based on the machine *d-q* equivalent circuit and phasor diagram. Fig. 2 shows an

This work was financially supported by Australian Research Council grant DP170103343.

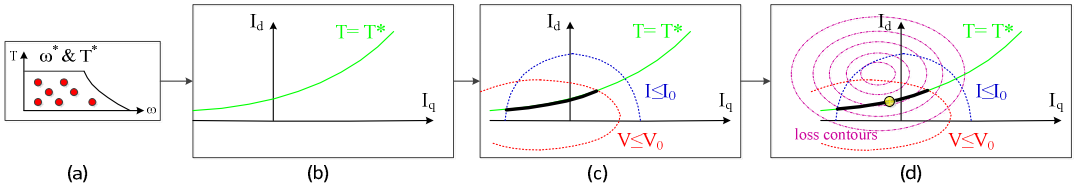

Fig. 1 Efficiency map calculation process.

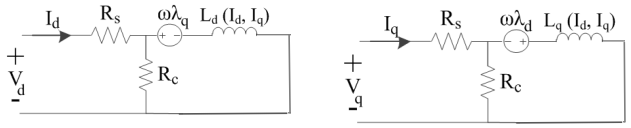

Fig. 2 IPM equivalent circuit used for efficiency calculation.

equivalent circuit of PM machines that uses the following parameters: stator resistance R_s, d- and q-axis inductances L_d, L_q, and magnet flux-linkage λ_m, which can be obtained from analytical calculations or from FE or measurement.

The d-q axis flux linkages are formulated as:

$$\lambda_d = \lambda_m + L_d I_d \text{ and } \lambda_q = L_q I_q \quad (1)$$

So, the resultant torque is formulated as:

$$T(I_d, I_q) = \frac{m}{2} p\left[\lambda_d I_q - \lambda_q I_d\right] \quad (2)$$

where p is the number of pole-pairs and m is the number of phases. The current limit (I_0) and voltage limit (V_0) constrain the torque value for a given speed.

$$\sqrt{I_d^2 + I_q^2} \le I_0 \quad \text{and} \quad \omega\sqrt{\lambda_d^2 + \lambda_q^2} \le V_0 \quad (3)$$

The next step towards calculating the efficiency map is obtaining the loss. The total loss is calculated as a sum of iron loss and copper loss. The analytical-based approaches usually assume that iron loss varies only with speed and generally use the open-circuit loss value. So, the total loss is formulated as:

$$P_{loss}(\omega) = 3\left(I_d^2 + I_q^2\right)R_s + P_{fe}(\omega) \quad (4)$$

Therefore, for any operating speed, efficiency is calculated as,

$$\eta(T, \omega) = \frac{T\omega}{T\omega + P_{loss}(T,\omega)} \quad (5)$$

Although this method is fast compared to the FE, it has a number of approximations and thus limited accuracy.

B. *Studied Traction Machines*

Two examples of 50-kW PM machines are considered in this paper, one an interior PM design (IPM) and the other a surface PM design (SPM) [5]. Both are designed for a traction application. Fig. 3 shows the cross-sections of the designs and Table I summarizes their parameters.

III. Flux Linkage and Torque Estimation

Under real operating conditions, the electrical machines shows some degree of saturation and cross-saturation. Under the cross-saturation condition (which is applicable to the most general case), the d- and q- axis flux linkages are functions of both d- and q- currents ($\lambda_q(I_d,I_q)$ and $\lambda_d(I_d,I_q)$). Fig. 4 shows the flux variation of the studied SPM and IPM machines under cross saturation, saturation, and linear conditions. The thick black lines show the λ_d when I_q=0 and λ_q when I_d=0 which are used in the saturation approximation method. In general, the d-axis flux linkage magnitude decreases with increasing I_q current. The effect of cross saturation is more pronounced for the SPM compared to the

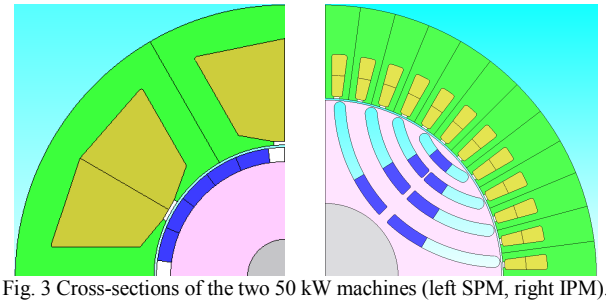

Fig. 3 Cross-sections of the two 50 kW machines (left SPM, right IPM).

TABLE I. SPECIFICATIONS OF 50-KW, 12 KR/MIN MOTORS [5].

	IPM	SPM
Key Dimensions		
- stator outer diameter	216 mm	
- stack length	170 mm	
- airgap length	0.7 mm	1 mm
Design Parameters		
- poles	4	4
- stator slots	48	6
- number of turns	24	24
- copper slot fill (copper/slot area)	40%	55%
Electrical Parameters		
- torque @ 360 A	164 Nm	240 Nm
- characteristic current (peak)	210 A	240 A
- stator resistance (130°C)	23 mΩ	20 mΩ

IPM. It means the d- and q-axis flux paths share more joint areas in the case of the SPM.

The equivalent-circuit method is used to estimate the machine performance using the saturated and linear inductance models. When taking saturation only into account, the d- and q- axis flux linkages are assumed only functions of their respective current ($\lambda_q(I_d)$ and $\lambda_d(I_q)$) which is the value of the λ_d when $I_q = 0$ and λ_q when $I_d = 0$. As the variation in flux-linkage due to cross-saturation is larger for SPM, it is expected that the saturation model will result in larger error compared to the IPM.

With highest level of approximation, the effect of saturation is ignored and machines are modeled as linear ($\lambda_d = L_d I_d$ and $\lambda_q = L_q I_q$, where L_d and L_q are constant). If the flux-linkages are not heavily saturated (like λ_q for SPM and λ_d for IPM), the linear model can provide acceptable estimation of the saturated results. For the IPM q-axis flux linkage, there are two possible estimates for the linear model. The first approximation (shown in blue) represents the unsaturated inductance while the second model (shown in green). The first model (blue) is selected as the linear approximation. To clarify the details of the d and q-axis flux behavior and the torque estimation under cross saturation, saturation, and linear conditions for SPM and IPM machines, Fig. 5 and 6 are presented. The maximum, minimum and zero d-axis flux and maximum q-axis flux are shown in black lines.

First consider the SPM machine in Fig. 5. The d and q-axis flux under cross-saturation condition (shown in the left columns) includes curved lines that are distributed unevenly.

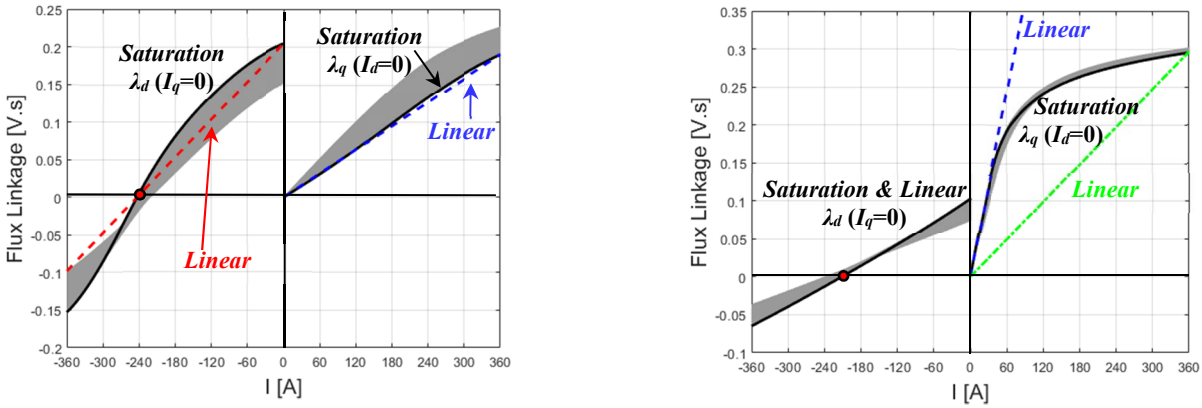

Fig. 4 *d*- and *q*-axis flux-linkage versus axis current curves showing cross-saturation (grey region) and approximations using saturation and linear estimates (lines) (left SPM, right IPM).

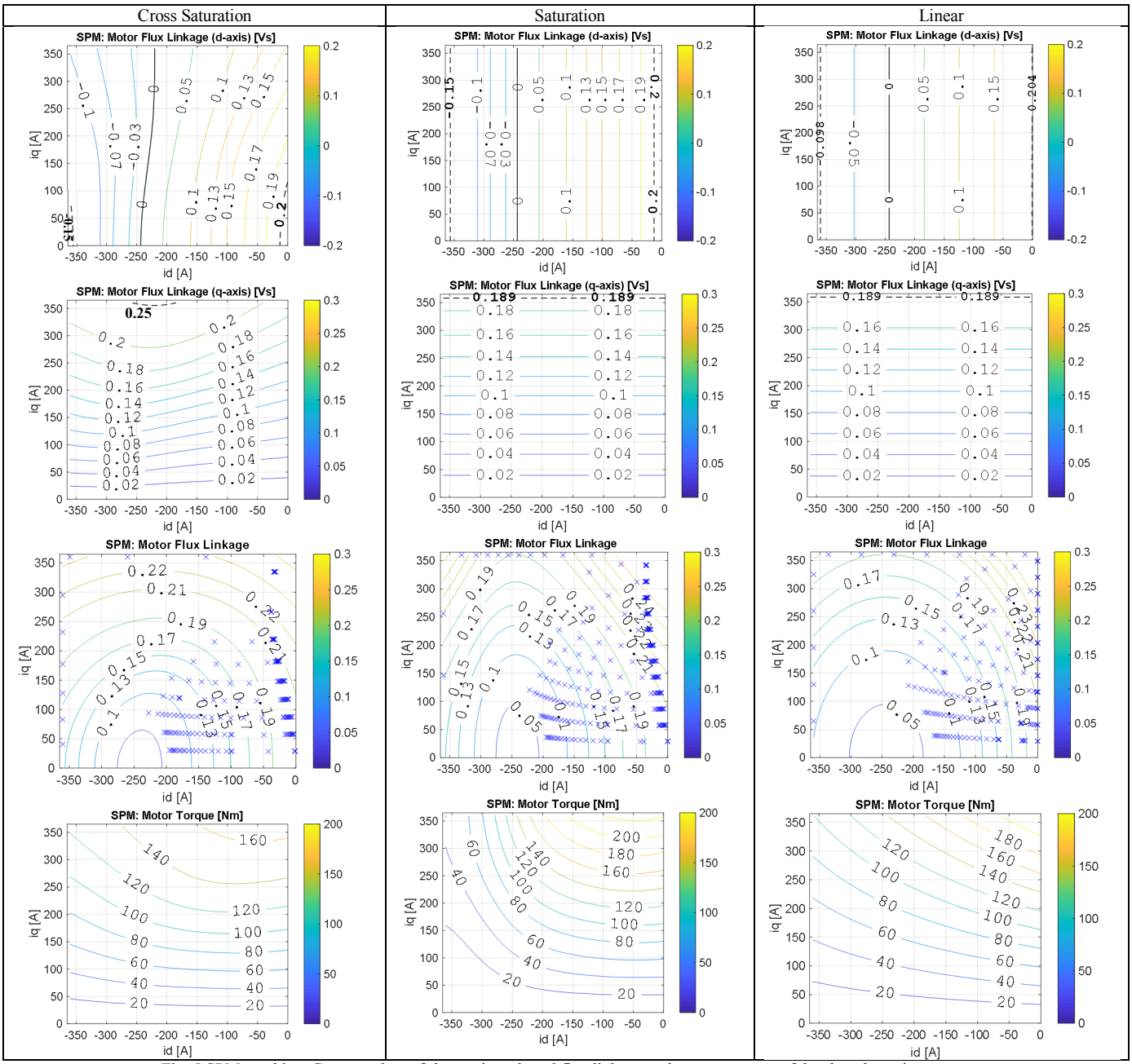

Fig. 5 SPM machine. Contour plots of *d*-, *q*-axis and total flux linkage and torque on axes of the *d*- and *q*-axis current.

So, the total flux-linkage contour plot has eccentric ellipses. By estimating the machine with a saturation only model (middle column), the flux-linkage curves become unevenly distributed lines and the total flux-linkages include

distorted ellipses. Under linear condition ($\lambda_d = L_d I_d$ and $\lambda_q = L_q I_q$) which means that L_d and L_q are constant, the d- and q-axis flux-linkage lines are equally spaced. Hence, as shown in the figure, the total flux-linkages are perfect ellipses (right column). The blue crosses in the flux contours show the operation regions (the points with minimum loss used to plot the efficiency map) in the I_d-I_q plane. In the actual model, the operation points are more concentrated in the -230A $\leq I_d \leq$ 0A range. The saturation operation points follow a similar trend with more points on the I_q=360A line while the linear operation points are shifted towards the y-axis.

The accuracy of the torque results is determined by the accuracy of the flux-linkage estimation method as it is the external product of the flux-linkage and current. The SPM torque is ideally only magnet torque and thus only a function of I_q, but in practice it is significantly affected by I_d due to cross- saturation. By comparing the torque values in the real and saturated models it can be concluded that the error is due to the estimation of the q-axis flux-linkage. As previously illustrated in Fig. 4, the difference between the saturated and linear models of the d-axis flux is significant which changes the resultant torque. The maximum and minimum flux values shown in the graphs provide a benchmark for the torque difference.

For the IPM motor (Fig. 6) the magnet torque is associated with I_q while the reluctance torque is the product of I_d and I_q. As the IPM machine does not have a high level of cross saturation, the estimated resultant torque from the saturation model has acceptable accuracy. However, the linear model provides inaccurate torque values at higher values of I_q due to the use of the unsaturated inductance.

The operation points of the IPM have a completely different trend compared to the SPM. The operation points for the actual and saturation models follow the same pattern and extend between the maximum to minimum I_d and 0 to 150 A for I_q. However, the operation points of the linear model are limited to lower values of I_q by the voltage boundary as the linear model overestimates the λ_q.

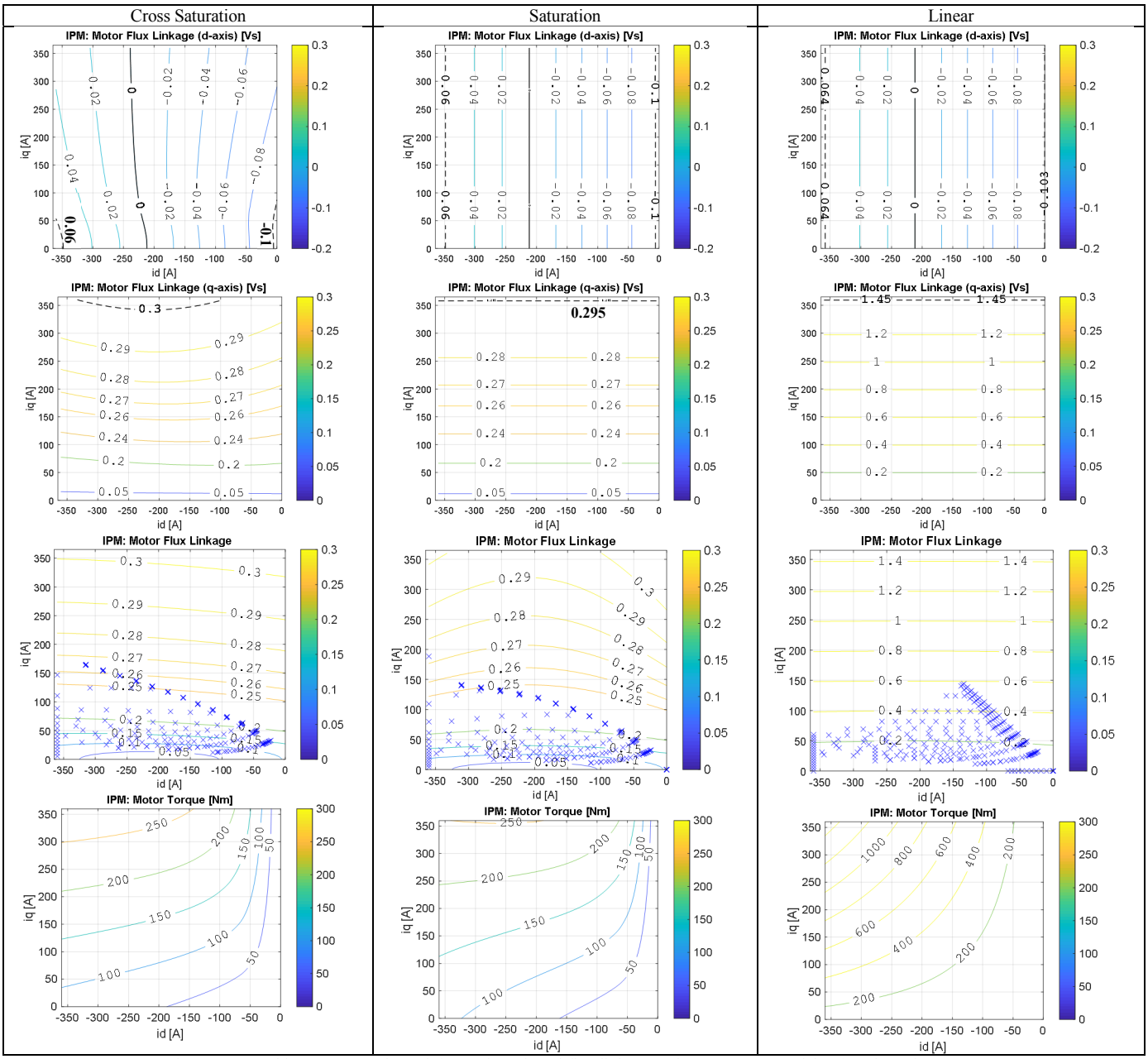

Fig. 6 IPM machine. Contour plots of d-, q-axis and total flux linkage and torque on axes of the d- and q-axis current.

Fig. 7 shows the effect of estimating the flux linkage using the saturation and linear models on the torque-speed capability curve. For the SPM, the saturation and linear flux methods overestimate the torque in the constant torque region by about 30% while they are more accurate at high speed (after 7000 rpm). In addition, with these approximations, the rated speed reduces from 3500 rpm in the real condition to about 3000 rpm in the other methods.

The capability curve estimation of the IPM shows the initial 4% underestimation of saturation model and 7% overestimation of the linear model in the constant torque region. Interestingly, the approximate capability curves converge to the actual graph in the constant power region indicating that these estimates are reliable at middle and high speed ranges. The rated speed of the linear model is similar to that of cross-saturation while it is slightly higher for the saturation model.

IV. Loss and Efficiency Estimation

A. Loss breakdown

Fig. 8 shows the loss plots as functions of I_d and I_q at the rated speed of 3,800 rpm, separated into the stator copper loss, the stator iron loss, the PM loss and the rotor iron losses. The copper loss is the dominant loss at the rated speed (Fig. 8(a)). By comparing the total flux-linkage shown in Fig. 6 with the stator iron loss in Fig. 8(b), it is noted that the shape of SPM stator iron loss plot follows the trend of its flux linkage however this is not the case for the IPM machine. This highlights the importance of considering the effect of cross-saturation when modelling iron loss using analytical

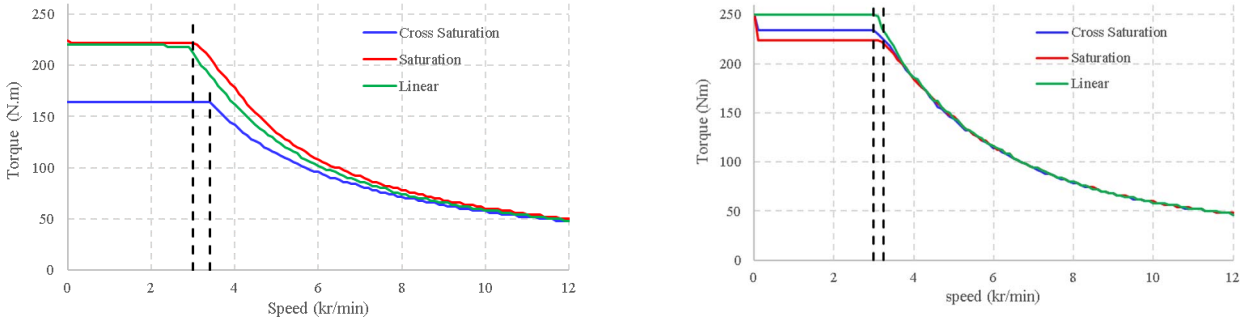

Fig. 7 Torque-speed envelope under cross-saturation, saturation, and linear conditions (left SPM, right IPM).

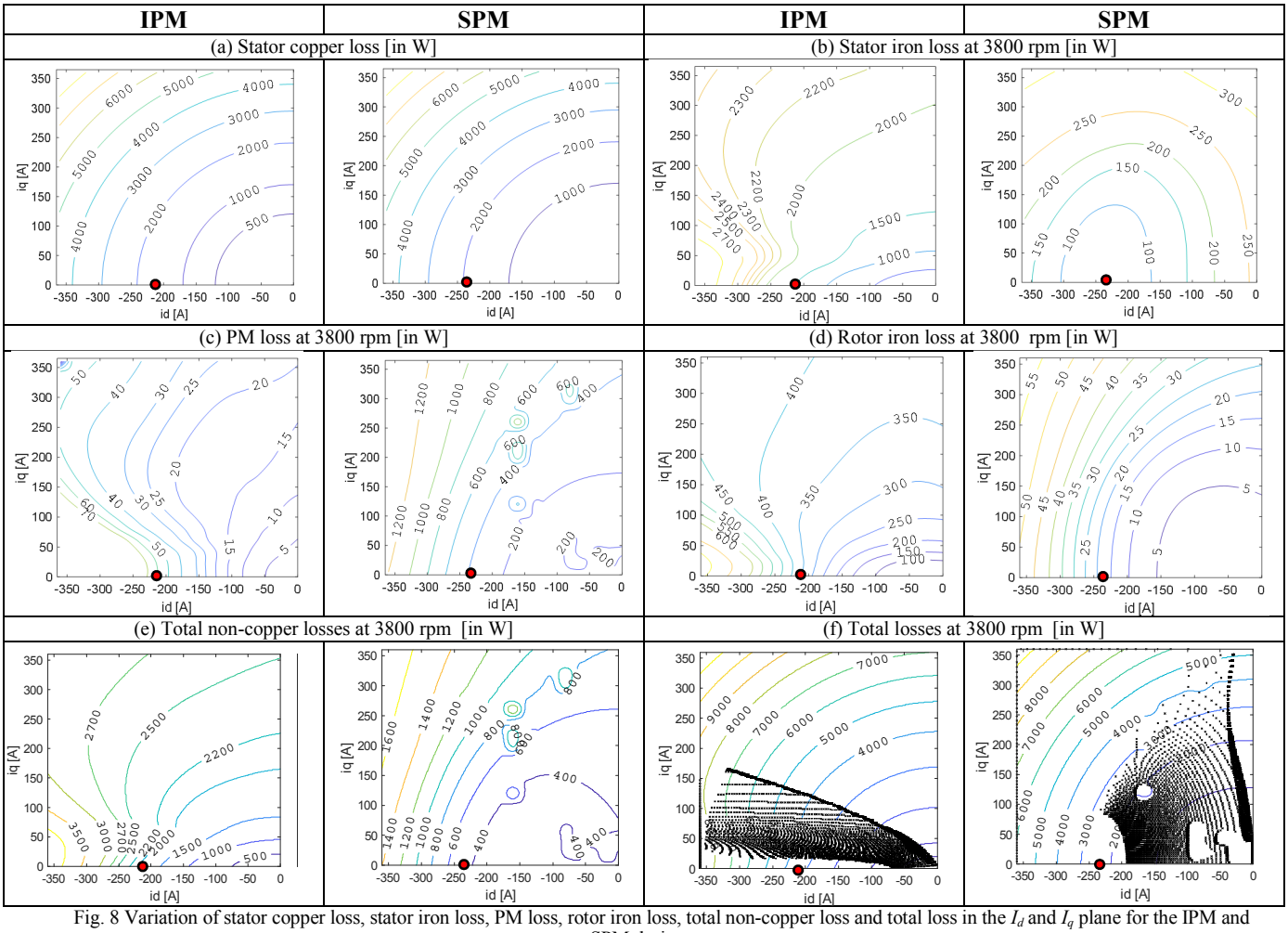

Fig. 8 Variation of stator copper loss, stator iron loss, PM loss, rotor iron loss, total non-copper loss and total loss in the I_d and I_q plane for the IPM and SPM designs.

approaches.

By comparing the value of the stator and rotor iron losses at the rated speed, it is concluded that rotor iron losses contribute less in total loss generation. The PM loss of the IPM machine is negligible while it is the dominant loss for the SPM machine. Figs. 8(e) and 8(f) are the non-copper losses and total losses, respectively, in which the (I_d, I_q) operating trajectories for maximum efficiency are indicated.

B. Open-circuit and short-circuit losses

An important feature of the PM machines is the characteristic current which corresponds to zero flux-linkage value. This is the *d*-axis flux linkage intercept which is 240 A for SPM and 210 A for IPM (shown with as a solid red circle in Fig. 8). Another important loss value is the open-circuit point. The losses corresponding to these two operating points represent the open-circuit and short-circuit losses of the machine.

One of the aims in this paper is to estimate the efficiency map using limited test results, instead of a full loss map based on the flux variation, and for this purpose the non-copper loss is considered solely a function of speed. This is the general approach used in the equivalent circuit based methods. As open-circuit (associated with $I_d = I_q = 0$) and short-circuit (associated with $I_d = -I_{char}$ @ $\lambda_d = 0$) are relatively simple loss tests to conduct.

Fig. 9 shows the iron (non-copper) losses of the SC/OC tests versus speed where the 3,800 rpm eddy current and hysteresis loss results are scaled with fundamental frequency [1]. This figure also highlights the operating trajectories of minimum iron losses (green areas). For the SPM, the OC loss is roughly the average of actual loss band while the SC loss overestimates the maximum real loss values by almost 30%. However, for the IPM the SC loss represents a more realistic average approximation of the real losses.

C. Loss map using OC and SC losses

Fig. 10 compares the OC and SC loss estimation of the total loss and shows their impact on the accuracy of efficiency map for SPM and IPM machines. The first column shows the actual calculated non-copper losses and efficiency map based on the values of (I_d, I_q). The second and third columns examine approximating the non-copper loss map using the results of the OC and SC loss tests which have only speed dependence. In the SC test, the SC current (I_{sc}) is approximated as the characteristic current, thus $I_d = -I_{sc}$ and $I_q = 0$. Therefore λ_d, I_q and voltage at any rotational speed are assumed to be zero. The SC test can be performed on PM machines designed for field-weakening operation where the SC current does not significantly exceed the rated current.

For the SPM, using both OC and SC loss curves resulted in fairly accurate loss estimation in the low speed range while the domain of 2% efficiency error is slightly extended in speed for the OC test. However, in the low torque high speed range, both methods had up to 10% error while the SC results had considerably poorer accuracy. The larger error in the high speed region is due to the importance of the loss variation with load which is ignored in both the OC and SC loss estimation.

For the IPM, the OC and SC estimates produce similar loss patterns at the higher levels of the constant torque region

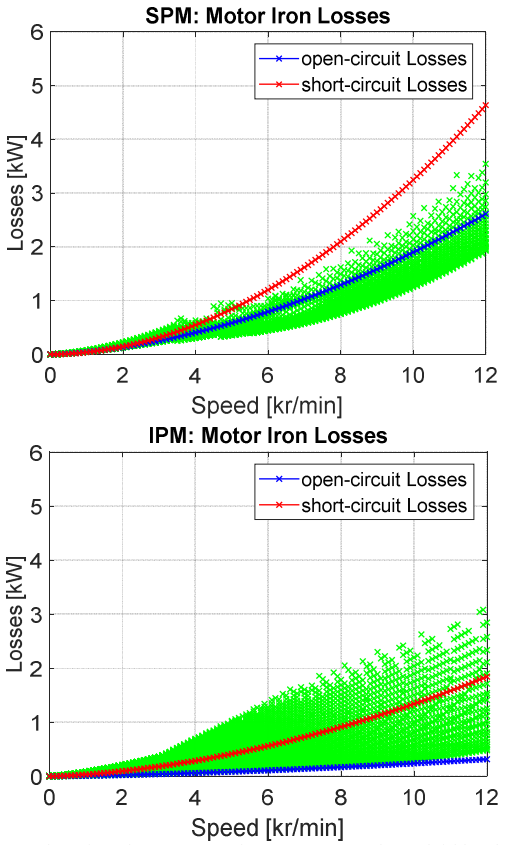

Fig. 9 Scatter plot of total non-copper loss versus speed overlaid by the short and open-circuit loss versus speed curves (top SPM, bottom IPM).

while for the high speed region the SC loss provided a more accurate estimate of the loss.

V. Flux and Loss Estimation

The goal of this paper is to estimate the efficiency maps using limited experimental tests. Therefore, in this section the effect of approximating the flux linkage characteristics using saturation and linear models (instead of cross-saturation) and OC and SC loss approximation methods (instead of the true loss variation with flux) for both SPM and IPM machines are presented and results are shown in Fig. 11.

First, consider the SPM machine. As mentioned before in Fig. 7, both saturation and linear flux approximation models overestimate the torque in the constant torque region (by almost 30%). Second, the saturation model has similar behavior under OC and SC tests and overestimates the efficiency map at the low speed, high torque region. However, the comparison between the constant torque and high speed range shows a maximum underestimate of 3% and 15% in the efficiency map for the OC and SC losses, respectively. Using the OC test results, the regions with ±2% errors covers more than 70% of the total torque-speed domain showing the saturation model and OC test provides acceptable approximation of the efficiency map for a wide speed range. Third, the linear model provides even less error in the efficiency map where almost 87% of the efficiency map is within ±2% error. This is not an intuitive result but by considering Fig. 4, it is seen that the saturation model approximates the maximum value of λ_d from the cross-saturation results while the linear λ_d passes almost

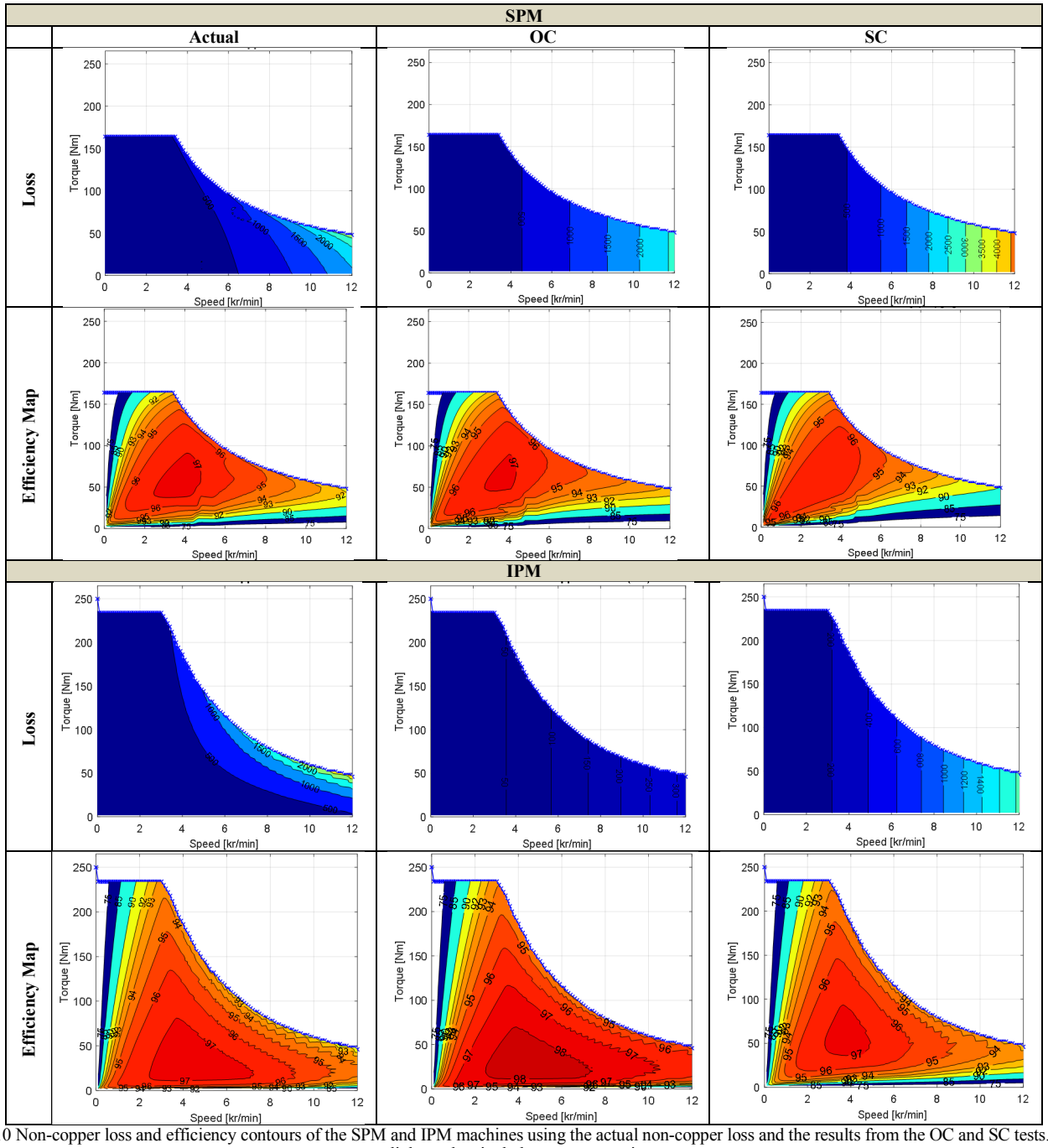

Fig. 10 Non-copper loss and efficiency contours of the SPM and IPM machines using the actual non-copper loss and the results from the OC and SC tests. Flux linkage data includes cross saturation.

through the middle of the maximum and minimum flux band.

It is noted that the non-copper loss is a function of flux so when the flux is estimated using saturation and linear models, it is necessary to obtain the new loss characteristics (specifically for the SC model). To achieve the new loss map for each flux estimation method, firstly a curve fit of the loss components (eddy current and hysteresis loss components of stator and rotor losses and also the PM losses) as a function of λ_d and λ_q are found. These functions are applied to the new flux estimation data to obtain the new iron loss characteristics which is essential in the SC test.

For the IPM, the saturation model slightly overestimates the maximum torque in the constant torque/low speed region while it converges to the real value at about 4 krpm. The OC loss estimation resulted in a maximum of 3% error for the efficiency map while this error is slightly higher for the SC loss model especially in the low torque region.

Last, the linear approximation of the IPM machine does not provide a realistic approximation of the efficiency map due to the large error in the λ_q estimation. Similar to the previous cases, the OC loss estimation provides less error compared to the SC loss.

VI. Conclusions

A detailed insight towards the efficiency map estimation based on the flux-linkage and loss estimation has been provided in this paper. It discussed the behaviour of an interior PM motor and also a surface-mounted PM motor under real cross-saturation condition as well as its estimation with saturation and linear models. The study includes the torque versus speed operating envelope of each machine with

regards to the various flux linkage models. This paper has extracted the efficiency map via open-circuit and short-circuit loss models and compared the results against that calculated using an extensive finite-element based mapping of flux-linkage and losses as a function of the *d*- and *q*-axis currents.

For the SPM, the OC loss is a reliable approach for approximating the real loss value in the low speed range with up to 2% error. However, in the low torque high speed range, this error reaches up to 10%. The SC test produced poorer accuracy especially at the high power, high speed region.

For the IPM, the OC and SC loss models produce similar loss patterns at the higher level of the constant torque region while at high speeds the SC loss provided more accurate estimation of the loss.

When the effect of iron loss and flux estimation were integrated, it is concluded that for both SPM and IPM machines the saturation approximation of the flux linkage provides a fairly accurate estimation of the efficiency map within ±2% error in the constant power region using the open-circuit loss. In the constant torque region the SPM showed 30% overestimation of the maximum torque in the low speed region. For the SPM with its high level of cross-saturation, the linear approximation actually reduces the error compared to the saturation model while for the IPM, the linear estimation is inaccurate due to the over estimation of the *d*-axis flux linkage.

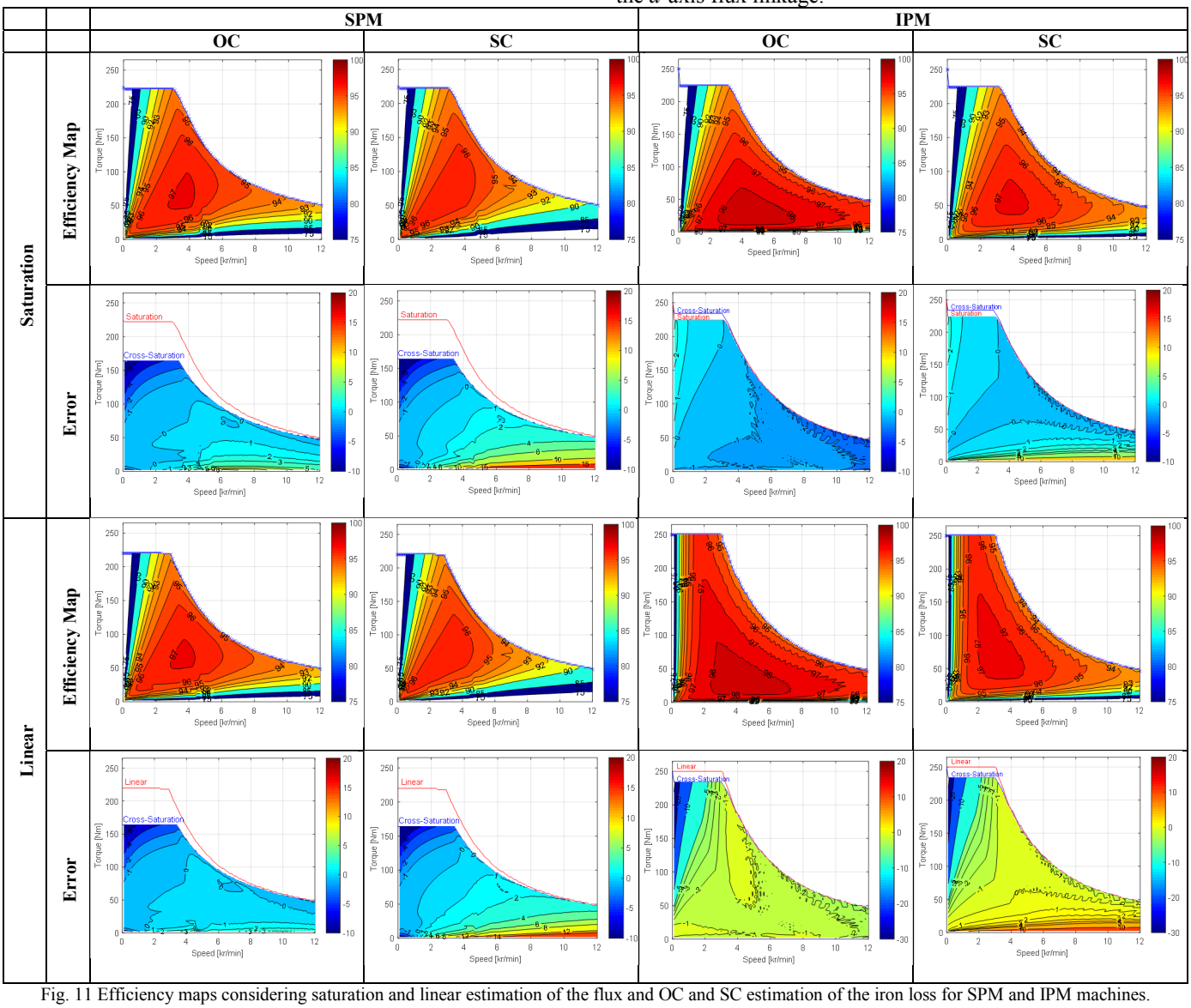

Fig. 11 Efficiency maps considering saturation and linear estimation of the flux and OC and SC estimation of the iron loss for SPM and IPM machines.

REFERENCES

[1] A. Mahmoudi, W. Soong, G. Pellegrino, and E. Armando, "Loss Function Modeling of Efficiency Maps of Electrical Machines," *IEEE Transactions on Industry Applications,* vol. 53, Sept.-Oct. 2017, pp. 4221 - 4231.

[2] A. Brune, P. Dück, B. Ponick, A. Kock, and M. Gröninger, "Evaluation of an efficiency-optimized calculation of PM synchronous machines' operating range using time-saving numerical and analytical coupling," in *Vehicle Power and Propulsion Conference (VPPC), 2012 IEEE*, 2012, pp. 32-35.

[3] S. Stipetic and J. Goss, "Calculation of efficiency maps using scalable saturated flux-linkage and loss model of a synchronous motor," in *Electrical Machines (ICEM), 2016 XXII International Conference on*, 2016, pp. 1380-1386.

[4] J. Goss, P. Mellor, R. Wrobel, D. Staton, and M. Popescu, "The design of AC permanent magnet motors for electric vehicles: A computationally efficient model of the operational envelope," 6th IET International Conference on Power Electronics, Machines and Drives 27-29 March 2012.

[5] C. Lu, S. Ferrari, and G. Pellegrino, "Two design procedures for PM synchronous machines for electric powertrains," *IEEE Transactions on Transportation Electrification,* vol. 3, pp. 98-107, 2017.